

AD-A159 102

APPLICATION OF THE SYSTEM IDENTIFICATION TECHNIQUE TO
GOAL-DIRECTED SACCA (U) NORTH DAKOTA STATE UNIV FARGO
DEPT OF ELECTRICAL AND ELECTRON J D ENDERLE JUL 85
USAFSAM-TR-85-37 F49620-82-C-0035

1/1

UNCLASSIFIED

F/G 6/16

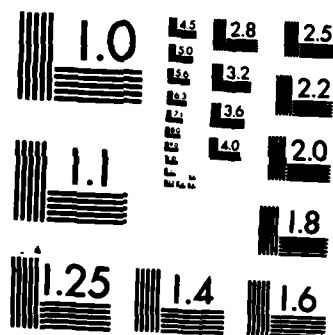
NL



END

FILED

DTIC



MICROCOPY RESOLUTION TEST CHART
NATIONAL BUREAU OF STANDARDS-1963-A

USAFSAM-TR-85-37

APPLICATION OF THE SYSTEM IDENTIFICATION TECHNIQUE TO GOAL-DIRECTED SACCADDES

John D. Enderle, Ph.D.

North Dakota State University
Fargo, North Dakota 58105

July 1985

Final Report for Period May 1984 - May 1985

Approved for public release; distribution is unlimited.

Prepared for

USAF SCHOOL OF AEROSPACE MEDICINE
Aerospace Medical Division (AFSC)
Brooks Air Force Base, TX 78235-5301



DTIC
ELECTE
SEP 13 1985
S D

85 9 11 001

AD-A159 102

DTIC FILE COPY

NOTICES


This final report was submitted by the Department of Electrical and Electronics Engineering, North Dakota State University, Fargo, North Dakota 58105, under contract F49620-82-0035, job order 7755-26-30, with the USAF School of Aerospace Medicine, Aerospace Medical Division, AFSC, Brooks Air Force Base, Texas. Dr. James W. Wolfe (USAFSAM/NGNS) was the Laboratory Project Scientist-in-Charge. The work was supported in part by Grant F49620-82-0035 from the Air Force Office of Scientific Research, Washington, D.C.

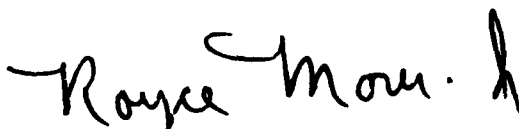
When Government drawings, specifications, or other data are used for any purpose other than in connection with a definitely Government-related procurement, the United States Government incurs no responsibility or any obligation whatsoever. The fact that the Government may have formulated or in any way supplied the said drawings, specifications, or other data, is not to be regarded by implication, or otherwise in any manner construed, as licensing the holder, or any other person or corporation; or as conveying any rights or permission to manufacture, use or sell any patented invention that may in any way be related thereto.

The Office of Public Affairs has reviewed this report, and it is releasable to the National Technical Information Service, where it will be available to the general public, including foreign nationals.

This report has been reviewed and is approved for publication.


JAMES W. WOLFE, Ph.D.
Project Scientist


DAVID R. JONES, M.D.
Supervisor



ROYCE MOSER, Jr.
Colonel, USAF, MC
Commander

UNCLASSIFIED

SECURITY CLASSIFICATION OF THIS PAGE

A159 102

REPORT DOCUMENTATION PAGE

1a. REPORT SECURITY CLASSIFICATION Unclassified			1b. RESTRICTIVE MARKINGS		
2a. SECURITY CLASSIFICATION AUTHORITY			3. DISTRIBUTION/AVAILABILITY OF REPORT Approved for public release; distribution is unlimited.		
2b. DECLASSIFICATION/DOWNGRADING SCHEDULE					
4. PERFORMING ORGANIZATION REPORT NUMBER(S)			5. MONITORING ORGANIZATION REPORT NUMBER(S) USAFSAM-TR-85-37		
6a. NAME OF PERFORMING ORGANIZATION Div. of Bioengineering, Dept. of Electrical & Electronics Engin.		6b. OFFICE SYMBOL (If applicable)	7a. NAME OF MONITORING ORGANIZATION USAF School of Aerospace Medicine (NGNS)		
6c. ADDRESS (City, State and ZIP Code) North Dakota State University Fargo, North Dakota 58105		7b. ADDRESS (City, State and ZIP Code) Aerospace Medical Division (AFSC) Brooks Air Force Base, Texas 78235-5301			
8a. NAME OF FUNDING/SPONSORING ORGANIZATION		8b. OFFICE SYMBOL (If applicable)	9. PROCUREMENT INSTRUMENT IDENTIFICATION NUMBER F49620-82-0035		
8c. ADDRESS (City, State and ZIP Code)		10. SOURCE OF FUNDING NOS.			
		PROGRAM ELEMENT NO.	PROJECT NO.	TASK NO.	WORK UNIT NO.
		62202F	7755	26	30
11. TITLE (Include Security Classification) APPLICATION OF THE SYSTEM IDENTIFICATION TECHNIQUE TO GOAL-DIRECTED SACCADDES					
12. PERSONAL AUTHOR(S) Enderle, John D.					
13a. TYPE OF REPORT Final Report		13b. TIME COVERED FROM May 1984 TO May 1985		14. DATE OF REPORT (Yr., Mo., Day) 1985, July	
				15. PAGE COUNT 27	
16. SUPPLEMENTARY NOTATION					
17. COSATI CODES			18. SUBJECT TERMS (Continue on reverse if necessary and identify by block number)		
FIELD	GROUP	SUB. GR.			
06	05		Saccadic Eye Movements		
14	02		Oculomotor System		
			System Identification		
19. ABSTRACT (Continue on reverse if necessary and identify by block number) System identification techniques were used to estimate muscle forces during horizontal saccadic eye movements in order to better understand the neuronal control strategy. The lateral and medial rectus muscle of each eye was modeled as a parallel combination of an active state tension generator with a viscosity and elastic element, connected to a series elastic element. The eyeball was modeled as a sphere connected to a viscosity and elastic element. The predictions of the model were shown to be in good agreement with the data. The results of extensive analysis did not support the existence of a postulated continuous-time external feedback control mechanism. Analysis of the data, however, did support a time optimal control strategy, a strategy which directs the eyeball to its destination in minimum time for saccades of all sizes.					
20. DISTRIBUTION/AVAILABILITY OF ABSTRACT UNCLASSIFIED/UNLIMITED <input checked="" type="checkbox"/> SAME AS RPT. <input type="checkbox"/> DTIC USERS <input type="checkbox"/>			21. ABSTRACT SECURITY CLASSIFICATION Unclassified		
22a. NAME OF RESPONSIBLE INDIVIDUAL James W. Wolfe, Ph.D.		22b. TELEPHONE NUMBER (Include Area Code) (512) 536-3201		22c. OFFICE SYMBOL USAFSAM/NGNS	



Accession For	
DTIC GRA&I	<input checked="" type="checkbox"/>
DTIC TAB	<input type="checkbox"/>
Unannounced	<input type="checkbox"/>
Justification	
By	
Distribution/	
Availability Codes	
Dist	Avail and/or Special
A-1	

APPLICATION OF THE SYSTEM IDENTIFICATION TECHNIQUE TO GOAL-DIRECTED SACCADDES

INTRODUCTION

Saccadic eye movements are among the fastest voluntary muscle movements the human body is capable of producing and are characterized by a rapid shift of gaze from one point of fixation to another. Although the purpose for such an eye movement is obvious, that is, to quickly redirect the eyeball to the target, the neuronal control strategy is not. For instance, does the word "quickly" in the previous sentence imply the most rapid movement possible, or simply a fast movement as opposed to a slow movement? This investigation uses system identification techniques to estimate muscle forces during horizontal saccadic eye movements in order to better understand the neuronal control strategy.

Until recently, models of the saccadic eye movement system involved a ballistic or preprogrammed control to desired eye position based on retinal error alone (1-4). Today, an increasing number of authors are putting forth the idea that goal-directed saccades are controlled by a local feedback loop that continuously drives the eye to the desired position. This hypothesis, first presented by Vossius (5) in 1960, did not start to gain acceptance until 1975 when Robinson (6) reexamined it. Robinson suggested that saccades originate from neural commands, which encode saccade velocity and duration, to the pulse generator that specifies the desired position of the eye rather than the preprogrammed distance the eye must be moved. The image of the internal representation of the current eye position is subtracted from the internal representation of the desired position, creating an error signal that completes the local feedback loop to generate the neural control signal. This neural pulse continuously drives the eye until the internal representation of the error signal is zero.

One of the basic tasks of this project is to investigate whether an external, continuous-time sensor feedback control mechanism operates during a saccadic eye movement. Studies by other investigators indicate that the

profile of a saccade can be altered up to 50 ms after target movement, and that visual information is processed continuously during this interval (7,8). Their results indicate that 50 ms after target movement, the saccade profile cannot be altered by altering the target location. This experiment attempts to verify their results by artificially maintaining a constant error throughout the saccade by moving the target the same distance the eyeball moves. Collewyn and Van der Mark (9), in their study of the slow phase of optokinetic nystagmus, used this method of artificially opening the feedback loop.

A second task in this project involves the investigation of a horizontal saccadic eye model presented by Enderle (10). Estimated values of the poles of the transfer function showed an increasing trend as target displacement increased. A number of reasons may account for this increase, a significantly nonlinear model and/or an inaccurate model, or poor initial estimates for the parameter values. The model for horizontal saccadic eye movements must be accurate since it will be used in sensitively assessing whether an external feedback control mechanism operates during saccades.

MODEL OF OCULOMOTOR PLANT

In developing Enderle's model for horizontal saccadic eye movements, equation 2 assumed that the time derivative of the antagonist tension was negligibly small (10). This assumption was a major factor in the resulting functional relationship between target displacement and poles of the transfer function. The initial parameter estimates, which will be discussed in the next section, also affect this relationship. Using Laplace variable analysis about the operating point or initial eye position, it is possible to derive the following new and more accurate model of horizontal saccadic eye movements appropriate for the system identification technique (11).

$$\delta(K_{ST}(F_{AG}-F_{ANT})+B_{ANT}\dot{F}_{AG}-B_{AG}\dot{F}_{ANT}) = \ddot{\theta} + P_3\ddot{\theta} + P_2\dot{\theta} + P_1\dot{\theta} + P_0\theta \quad (1)$$

This model modifies and corrects the linear homeomorphic model by Bahill et al. (4). Implementing this model in the parameter estimation routine resulted in an excellent match between model prediction and the data.

Figure 1 presents a block diagram of the saccadic eye movement system which functions as one element within the overall system controlling all oculomotor movements. The saccadic eye movement system consists of three components: (1) the controller (i.e., the agonist and antagonist active state tension generators), (2) the oculomotor plant, and (3) the feedback element H. The oculomotor plant, indicated by the section within the dashed lines in Figure 1, is based on the Laplace transform of equation 1. Note that under an assumed ballistic control of saccadic eye movements, time delays in the feedback element cause this system to operate in an open-loop mode. If, in fact, an external continuous-time feedback control mechanism exists, then opening the feedback loop causes the system to overreact because of the constant error present at the input.

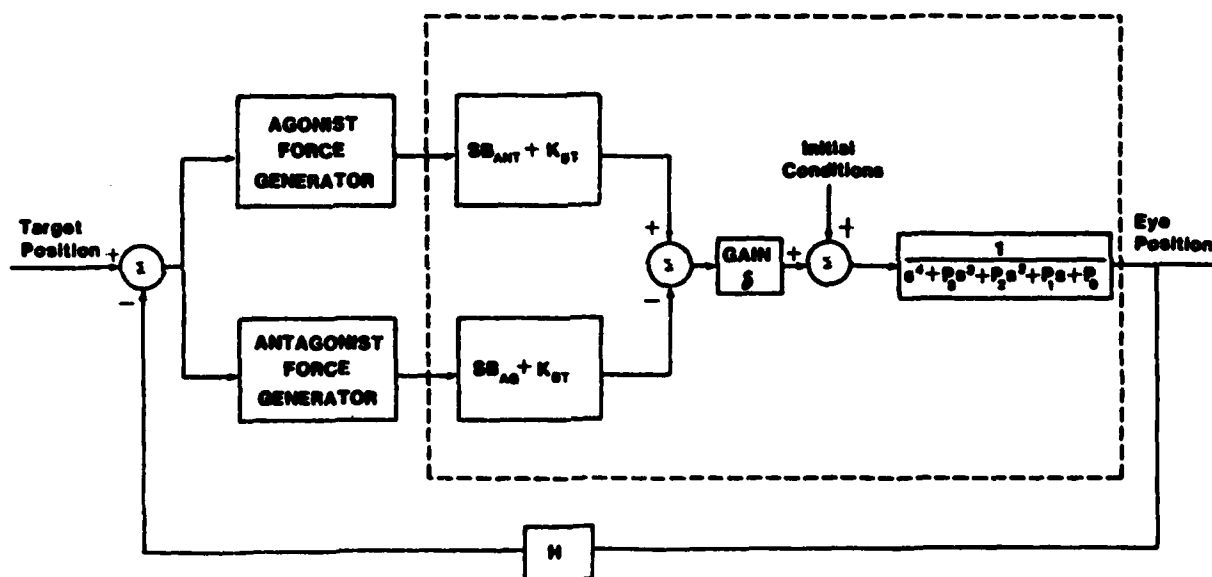


Figure 1. A block diagram of the oculomotor plant. The section of the diagram within the dashed lines is the modified linear homeomorphic model. The feedback element H is unity.

Since the derivation of the modified linear homeomorphic model requires no assumptions concerning the saccadic active state tensions, any type of control signal may be used. For example, investigators may use this model when examining alternatives to the pulse-step muscle force. If a continuous-time external feedback control mechanism exists, then a new waveform could be

postulated for the active state tension. This waveform could then be revised based on the predicted response of the modified linear homeomorphic model.

The mechanical components of the model are connected so that the active state tension rate of change, together with the actual active state tensions, drives the eyeball to its final position. Consider the low-pass filtered pulse-step active state tension signals presented in Figure 2. During the initial pulse phase of the trajectory, the agonist active state tension drives the eyeball and the antagonist active state tension restrains the eyeball. Since the antagonist active state tension falls to zero during this interval, then the antagonist active state tension rate of change, \dot{F}_{ANT} , is negative and, as indicated by equation 1, acts to drive the eyeball along with the agonist force, F_{AG} , and the agonist rate of change force, \dot{F}_{AG} . As a result, a greater force propels the eyeball than if only the agonist and antagonist active state tensions are used, as shown in the plant input curves of Figure 2. This result agrees with the tension data recorded for horizontal saccadic eye movements (12,13). After the pulse phase of the trajectory, the agonist active state tension falls to a steady state value, resulting in a negative agonist active state tension rate of change, \dot{F}_{AG} . Thus, according to equation 1, the agonist rate of change force, \dot{F}_{AG} , acts to restrain the eyeball with the antagonist force, F_{ANT} , and the antagonist rate of change force, \dot{F}_{ANT} . As shown for the plant input curves in Figure 2, the resultant forces act like a dynamic brake which is reduced to zero as the eyeball reaches its destination.

SYSTEM IDENTIFICATION TECHNIQUE

Parameter estimates for the oculomotor system model presented in the previous section are found using the system identification technique as described by Enderle (10,14). The system identification technique is a frequency response method. Ideally, the transfer function is equal to the ratio of the Fourier transform of the output to the system input. For the oculomotor system, the transfer function is calculated from the fast eye response to a step target displacement. Unequal time delays and eye displacements from saccade-to-saccade for the same target displacement, make it impossible to use averaging techniques to reduce the effects of measurement

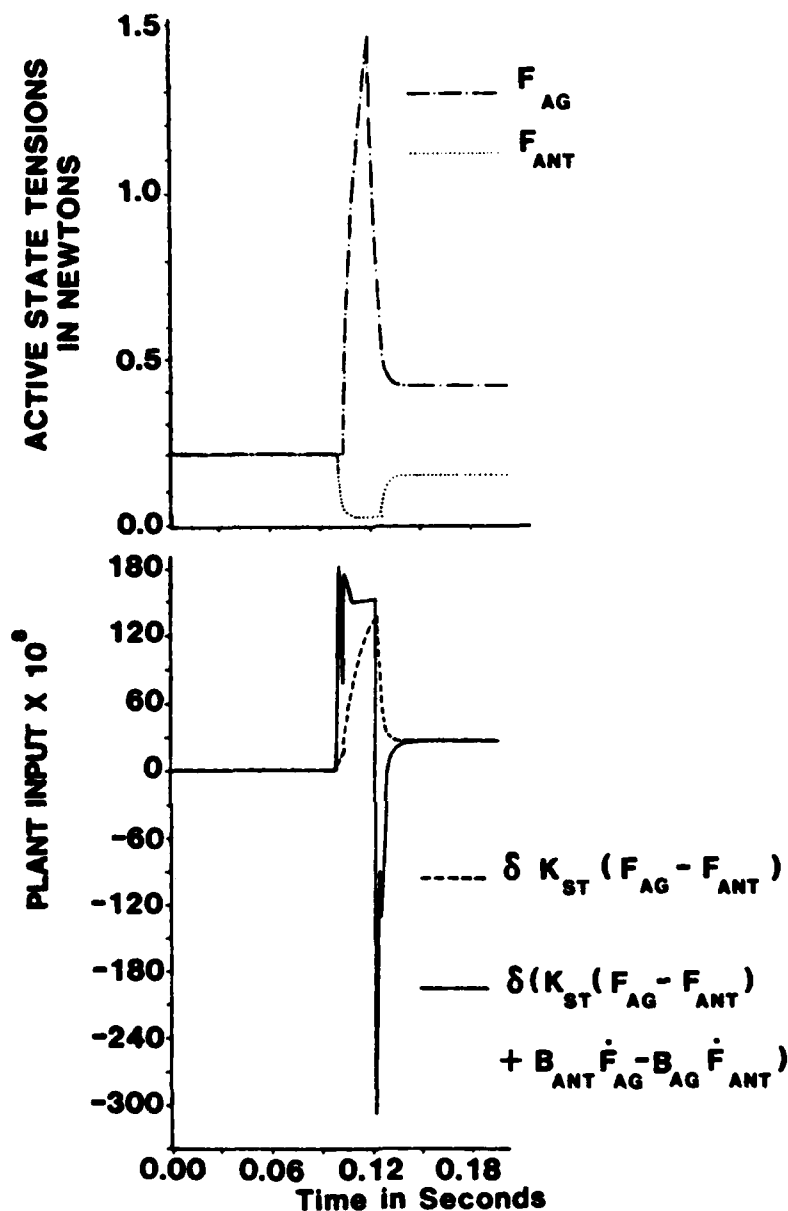


Figure 2. Transformation of the active state tensions by the numerator terms of the oculomotor plant. One diagram shows the assumed low-pass filtered pulse-step waveform of the agonist and antagonist active state tensions initiated at 100 ms. The antagonist pulse circumscribes the agonist pulse by 3 ms on each end. Parameter values are from Bahill et al. (4) for simulating a 10° horizontal saccadic eye movement. The other diagram shows a partial and full transformation of the active state tensions by the numerator terms of the oculomotor plant.

noise. Fortunately, the measurement noise is small relative to the input and output signals, so the second method described by Otnes and Enochson is used (15). The fast eye response measurements are first filtered using a Butterworth low-pass filter with a half-power point at 125 Hz. Transforming the filtered measurements directly by the Fast Fourier algorithm resulted in distortion due to truncation, since the signal did not go to zero at steady state. This problem is circumvented by subtracting the steady state value from each sample, passing this signal through a Kaiser window, packing with zeros, and Fast Fourier transforming the modified signal. The Fourier transform of the fast eye response is equal to the Fast Fourier transform of the modified signal plus the Fourier transform of the unit step with amplitude equal to the steady state value. The input signal is the Fourier transform of the unit step function with amplitude equal to the steady state value. Parameter estimates for the oculomotor model are calculated using the conjugate gradient search program similar to Seidel's, which minimizes the integral of the absolute value of the error squared between the model and the data (16).

Data were collected from subjects seated before a target display of seven small red light-emitting diodes (LED), each separated by 5° . The subject's head was restrained by a bite bar. The subject was instructed to follow the "jumping" target which moved from the center position to any of the other LEDs and returned to the center position. Target position order and time interval between displacements were randomized. Data were only recorded for the initial displacement from the center position.

Horizontal eye movements were recorded from each eye using an infrared signal reflected from the anterior surface of the cornea-scleral interface with instrumentation described by Engelken et al. (17). Signals for both eyes tracking were digitized using the analog/digital converter of the DECLAB PDP 11/34 computer and stored in disk memory. These signals were sampled at a rate of 1000 samples per second for one-half second.

Figure 1 presents a block diagram of the oculomotor system, which is suitable for the case of a ballistic controller, or as indicated, with an external continuous-time feedback control configuration. Under the assumption of ballistic control, the system operates in an open-loop mode due to time delays in the feedback element. Under the assumption of an external continuous-time controller during experiments in which the feedback loop is

artificially opened, the system also operates in an open-loop mode. Thus, the analysis of the data is performed with an open-loop system regardless of the type of control assumed operating. However, the signals describing the agonist and antagonist force generators are quite different, dependent on the type of controller.

The following low-pass filtered pulse-step waveforms describe the agonist and antagonist active state tensions under an assumed ballistic control mechanism:

$$F_{AG}(t) = F_{AGO}u(t) + (F_{AGP} - F_{AGO})(1 - \exp\{-(t - t_p)/\tau_{ac}\})u(t - t_p) - (F_{AGP} - F_{AGS})(1 - \exp\{-(t - t_p - t_d)/\tau_{de}\})u(t - t_p - t_d),$$

$$F_{ANT}(t) = F_{ANTO}u(t) - F_{ANTO}(1 - \exp\{-(t - t_p)/\tau_{de}\})u(t - t_p) + F_{ANTS}(1 - \exp\{-(t - t_p - t_d)/\tau_{de}\})u(t - t_p - t_d),$$

where

- F_{AGO} = initial magnitude of the agonist active state tension
- F_{AGP} = pulse magnitude of the agonist active state tension
- F_{AGS} = step magnitude of the agonist active state tension
- F_{ANTO} = initial magnitude of the antagonist active state tension
- F_{ANTS} = step magnitude of the antagonist active state tension
- t_p = latent period, the time interval between the target movement and the start of the eye movement
- t_d = duration of the agonist pulse active state tension
- τ_{ac} = activation time constant
- τ_{de} = deactivation time constant.

The steady state antagonist active state tension terms, F_{ANTO} and F_{ANTS} , are removed from the analysis since

$$F_{ANTO} = F_{AGO} - P_o \theta(0)/(\delta K_{ST})$$

and

$$F_{ANTS} = F_{AGS} - P_o \theta(\infty)/(\delta K_{ST})$$

according to equation 1. If either active state tension is less than zero, it is set equal to zero.

Physiological data was used to estimate all of the initial parameter estimates (4,13,18). Specifically

$K = 66.4 \text{ N/m}$	(Robinson)
$K_{LT} = 32. \text{ N/m}$	(Robinson)
$K_{SE} = 125 \text{ N/m}$	(Collins)
$B_{AG} = 3.5 \text{ N s/m}$	(Bahill)
$B_{ANT} = 1.66 \text{ N s/m}$	(Bahill)
$B = 3.1 \text{ N s/m}$	(Collins)
$J = 2.2 \times 10^{-3} \text{ N s}^2/\text{m}$	(Robinson)

The value of K is determined from the steady state agonist and antagonist muscle tensions

$$T_{AG} - T_{ANT} = Kx$$

where

$$T_{AG} = 17 + \theta \text{ g tension} \quad (2)$$

and

$$T_{ANT} = 17 - 0.3 \theta \text{ g tension}$$

from Figure 1 of Robinson et al. (18). The value of the muscle viscosity terms reported by Bahill et al. are modified according to their incorrectly derived result (4).

$$B_{AG} = K_{ST} B_{AG} / K_{SE}$$

and

$$B_{ANT} = K_{ST} B_{ANT} / K_{SE}$$

Substituting these values into the expressions for δ , P_0 , P_1 , P_2 and P_3 found in Enderle et al. (11), yields

$$\begin{aligned} \delta &= 5.0938109 \times 10^7 \\ P_3 &= 1.548 \times 10^3 \\ P_2 &= 3.4455 \times 10^5 \\ P_1 &= 1.9724 \times 10^7 \\ P_0 &= 2.2631 \times 10^8 \end{aligned}$$

The initial estimates for the four real eigenvalues as determined from the characteristic equations for this system are -15.27, -66.1, -173.36, and -1293.28. Now, the steady state active state tensions, F_{AGO} , F_{AGS} , are computed from

$$F_{AG} = \frac{K_{ST}}{K_{SE}} T_{AG} + K_{LT}(x - x_{P1}) \quad (3)$$

derived from Figure 1 in Enderle et al. (11). Substituting equation 2 into equation 3 with x_{P1} equal to 3.14 mm (assumed from Robinson (18)) yields

$$F_{AG} = .1089 + .01850 N$$

The initial estimate of the pulse magnitude of the active state tension, F_{AGP} , is 0.9806 (a maximum innervation signal of 100 g) (13).

The initial estimate of the duration of the agonist pulse active state tension is estimated directly from the data. The maximum velocity is computed using a two-point central difference derivate method (19). The initial estimate of t_p is then the time interval between the start of the saccade and the time at maximum velocity.

The initial estimate of the deactivation time constant is also estimated directly from the data as the time interval between maximum velocity and the end of the saccade divided by 4. The activation time constant equals 2 ms (20).

Great care was exercised in evaluating initial parameter estimates, since large differences from the true values could cause the estimation routine to converge to suboptimal and nonphysiologically consistent results. The precision of the parameter estimation routine results presented in Figures 3 and 4 for a 10° target movement are typical for the three subjects tested. There was no significant trend in the values of the eigenvalues with target displacement and the estimates correlated well with their physiological data derived values. Table 1 lists the final estimated values for the eigenvalues for target displacements of 5, 10, and 15° for one of the subjects.

EXTERNAL FEEDBACK CONTROL MECHANISM

Experiments were conducted in which the hypothesized continuous-time external feedback control mechanism was artificially opened. Data were collected on three subjects in two stages. First stage data consisted of natural saccades, elicited from target displacements of -15 to 15° . The second stage consisted of data collected by artificially maintaining a constant error of 5° throughout the saccade by moving the target (under

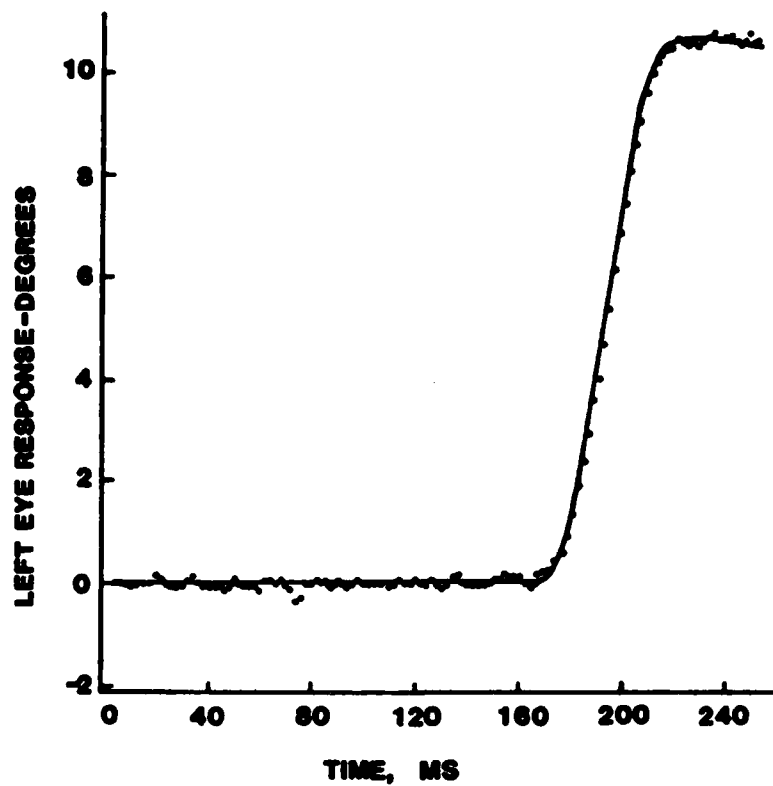


Figure 3. Time response for a 10° saccadic eye movement.

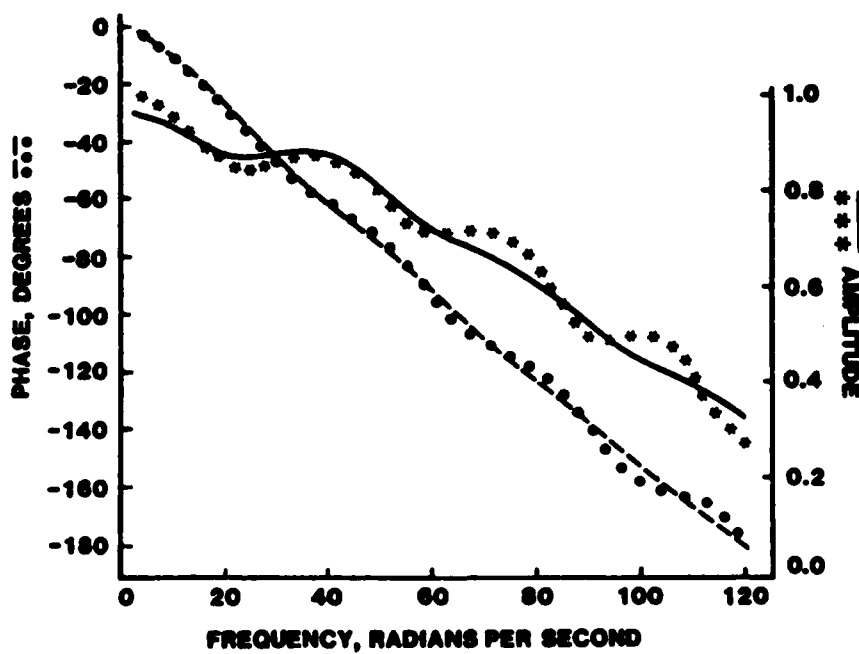


Figure 4. Frequency response for a 10° saccadic eye movement.

TABLE 1. FINAL PARAMETER ESTIMATES FOR THE FOUR REAL EIGENVALUES FOR TARGET DISPLACEMENTS OF 5, 10, AND 15° LEFT OF CENTER POSITION

		TARGET DISPLACEMENTS		
		<u>5°</u>	<u>10°</u>	<u>15°</u>
LEFT EYE	Eigenvalue 1	-14.4	-13.9	-13.7
	Eigenvalue 2	-83.8	-84.4	-93.6
	Eigenvalue 3	-190.9	-174.6	-157.4
	Eigenvalue 4	-1298.7	-1283.2	-1259.4
RIGHT EYE	Eigenvalue 1	-14.8	-14.4	-12.35
	Eigenvalue 2	-80.8	-84.9	-88.2
	Eigenvalue 3	-185.8	-165.4	-160.1
	Eigenvalue 4	-1302.2	-1261.6	-1223.7

computer control) the same distance the eyeball moved. This type of movement will be referred to as the modified target trajectory. The experiment started by the target moving $\pm 5^\circ$. The subject responded by following the jumping target. Instantaneously, as the eyeball moved, the target moved the same distance. Significant differences in saccade profile between the two stages would indicate the possible existence of an external feedback mechanism. Data was first analyzed using the two-point central difference method, and then using the system identification technique.

The results of the analysis of the data on the three subjects using the two-point central difference method are contained in the Appendix. Analysis results did not support the postulated continuous-time external feedback control mechanism. However, the time interval from the start of the saccade to the time at peak velocity for subjects 2 and 3 did show marked variation ranging from 21 ms to 8 ms. Most of the values were clustered about evenly into two groupings of 16 ms and 10 ms. These time interval results are plotted in Figure 5. It is interesting to note that the 5° movements elicited under natural conditions were always in the larger time interval grouping of 16 ms for each of the three subjects. It is speculated that if there were a continuous-time external feedback control mechanism, then both the time

interval and the final eye displacement would have been much larger than under normal conditions.

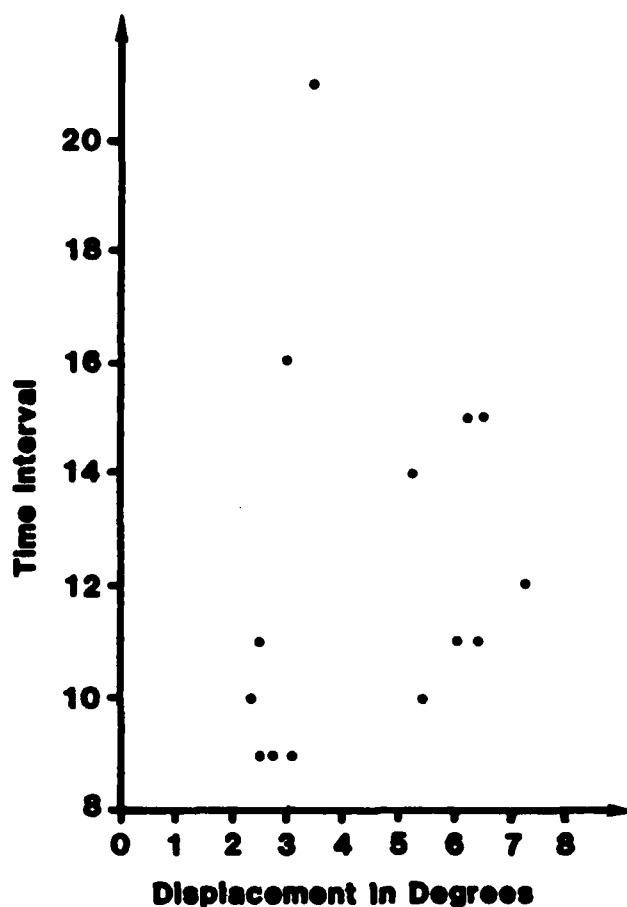


Figure 5. The time interval from the start of the saccade to the time at peak velocity vs absolute value of displacement for subject 2.

The results of the analysis of the data on the three subjects using the system identification technique confirmed the previous findings. Additionally, estimates of the pulse magnitude of the agonist active state tension F_{AGP} were clustered about evenly into two groupings, corresponding to the previous groupings, 0.95 N and 0.85 N. These results are plotted in Figure 6. The estimated pulse magnitude for the agonist active state tension as a function of displacement for the natural saccades is illustrated in

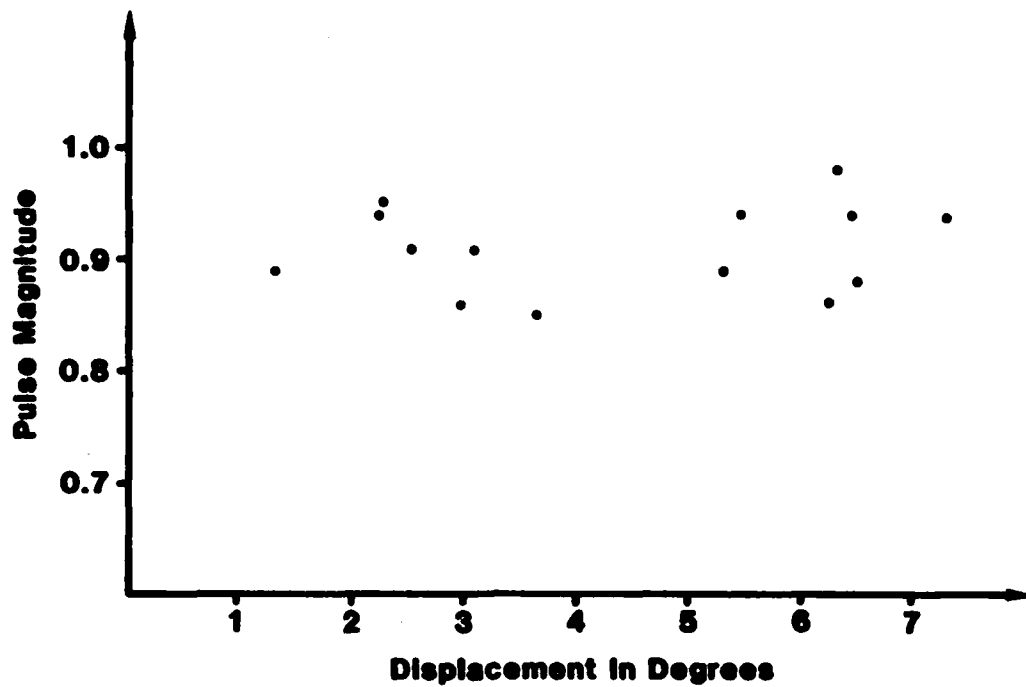


Figure 6. The estimated values of the pulse magnitude of the agonist active state tension vs absolute value of displacement for subject 3 during the stage 2 experiment.

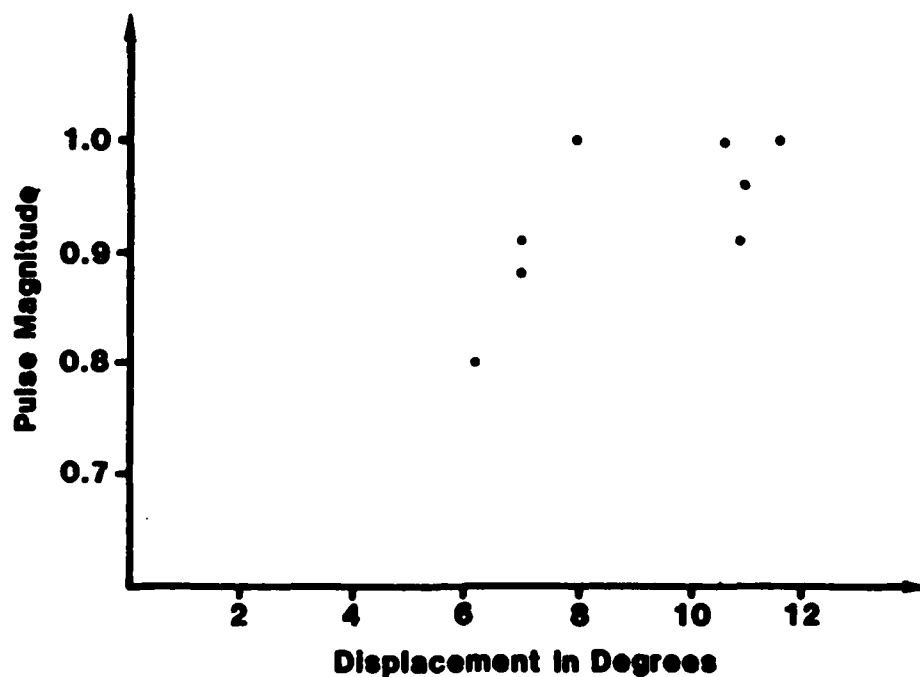


Figure 7. The estimated values of the pulse magnitude of the agonist active state tension vs absolute value of displacement for subject 3 during the stage 1 experiment.

Figure 7. One pronounced feature evident from these two graphs is that there does not appear to be a strong relationship between pulse magnitude and displacement. In fact the variation in F_{AGP} seen in Figure 6 is approximately the same size variation seen in Figure 7. Apparently the magnitude of the agonist pulse is maximum, regardless of the amplitude of the saccade, and only the duration of the agonist pulse affects the size of the saccade. Under these conditions, the eyeball is driven to its destination in minimum time for saccades of all sizes (21).

CONCLUSION

The conclusions obtained during the performance of this project indicate that the saccadic eye movement system operates under a time optimal control strategy without continuous-time external feedback sensory information. The implication that the eyeball is directed to its destination in minimum time for saccades of all sizes certainly deserves additional attention, considering the small number of subjects tested. This new hypothesis certainly should be investigated further in light of the current theory on the neuronal control of saccadic eye movements. Particular attention should be paid to the large variation seen with saccades of the same size. Furthermore, the importance of the second phase of the saccade, that is, when the agonist pulse is falling to its steady state value, must be understood in relation to the time optimal approach.

REFERENCES

1. Westheimer, G. Mechanism of saccadic eye movements. *Arch Ophthalmol* 52:710-723 (1954).
2. Young L.R., and L. Stark. Variable feedback experiments testing a sampled data model for eye tracking movements. *IEEE Trans Human Factors Electronics* 4:71-84 (1973).
3. Robinson, D.A. Models of the saccadic eye movement control system. *Kybernetik* 14:71-84 (1973).
4. Bahill, A.T., J.R. Latimer, and B.T. Troost. Linear homeomorphic model for human movement. *IEEE Trans Biomed Eng* BME-27:631-639 (1980).
5. Vossius, G. The system of eye movement. *Z Biol* 112:27-57 (1960).
6. Robinson, D.A. Oculomotor control signals, in *Basic Mechanisms of Ocular Motility and their Clinical Implications*, pp.337-378. G. Lennerstrand and P. Bach-y-Rita (eds.). Oxford: Pergamon Press, 1975.
7. Barmack, N.H. Modification of eye movements by instantaneous changes in the velocity of visual targets. *Vision Res* 10:1431-1441 (1970).
8. Wheelless, L.L., R.M. Boynton, and G.J. Cohen. Eye-movement responses to step and pulse-step stimuli. *J Opt Soc Am* 56:956-960 (1966).
9. Collewijn H., and F. van der Mark. Ocular stability in variable visual feedback conditions in the rabbit. *Brain Research* 36:47-57 (1972).
10. Enderle, J.D. Modeling and tracking saccadic eye movements. Participant's Final Report, 1982 USAF Summer Faculty Research Program sponsored by Air Force Office of Scientific Research conducted by Southeastern Center for Electrical Engineering Education under Grant F496-20-82-C-0035, September 1982.
11. Enderle, J.D., J.W. Wolfe, and J.T. Yates. The linear homeomorphic saccadic eye movement model-a modification. *IEEE Trans Biomed Eng* BME-31(11):717-720 (1984).
12. Collins, C.C. The human oculomotor control system, in *Basic Mechanisms of Ocular Motility and their Clinical Implications*, pp. 145-180. G. Lennerstrand and P. Bach-y-Rita (eds.). Oxford: Pergamon Press 1975.
13. Collins, C.C., D.M. O'Meara, and A.B. Scott. Muscle tension during unrestrained human eye movements. *J Physiol* 245:351-369 (1975).
14. Enderle, J.D. Estimation of saccadic eye movement muscle forces using system identification techniques, pp. 267-270. Presented at Second Southern Biomedical Engineering Conference, San Antonio, Texas, September 1983.

15. Otnes, R.K., and L. Enochson. Digital Time Series Analysis. N.Y.:John Wiley 1972.
16. Seidel, R.C. Transfer-function-parameter estimation from frequency-response data - a FORTRAN program. NASA-TMX-3286, 1975.
17. Engelken, E.J., K.W. Stevens, J.W. Wolfe, and J.T. Yates. A limbus sensing eye movement recorder. USAFSAM-TR-84-29, July 1984.
18. Robinson, D.A., D.M. O'Meara, A.B. Scott, and C.C. Collins. Mechanical components of human eye movements. J Appl Physiol 26:548-553 (1969).
19. Bahill A.T., and J.D. McDonald. Frequency limitations and optimal step size for the two-point central difference derivative algorithm with applications to human eye movement data. IEEE Trans Biomed Eng BME-30(3):191-194 (1983).
20. Robinson, D.A. Models of mechanics of eye movements, in Models of Oculomotor Behavior and Control, pp. 21-41. B.L. Zuber (ed.). Boca Raton, Florida: CRC Press 1981.
21. Enderle, J.D., J.W. Wolfe, and J.T. Yates. Optimal control of saccadic eye movements, pp.143-148. Presented at Twenty-First Annual Rocky Mountain Bioengineering Symposium, Boulder, Colorado, April 1984.

APPENDIX

ANALYSIS RESULTS

The two-point central difference analysis results on three subjects for natural and modified target trajectory saccade data are shown in Tables A-1 through A-6.

List of Symbols

Saccade - distance the target moved

Left and Right Displacement - the distance the left and right eye moved in response to the target displacement (degrees)

IC - initial position of the eyeball (degrees)

TD - time from the start of the saccade to the time at peak velocity (ms)

DUR - duration of the saccade (ms)

TP - time at which the saccade started (ms)

PV - peak velocity of the saccadic eye movement (degrees/second)

DIST - eye position at the time of peak velocity (degrees)

TABLE A-1. MODIFIED TARGET TRAJECTORY DATA
FOR THE LEFT EYE OF SUBJECT 1

SACCADE	DISPLACEMENT	IC	TP	TD	DUR	PV	DIST
5°L	5.29	.61	141	16	24	272	4.5
5°L	6.12	.54	212	17	26	342	5.0
5°R	-3.97	.48	164	11	31	-235	-1.6
5°L	6.12	.54	167	22	33	320	4.8
5°R	-4.42	.9	196	18	33	-272	-2.4
5°R	-4.49	.67	198	20	41	-240	-3.1
5°R	-4.2	.9	192	20	32	-251	-2.8
5°L	6.02	.96	193	19	26	283	5.4
5°L	6.38	1.15	238	14	28	294	4.3
5°R	-2.05	1.57	157	20	30	-176	-1.3
5°L	6.38	1.06	206	19	26	368	5.9
5°R	-3.01	1.22	141	15	18	-224	-1.5
5°R	-3.49	1.35	149	15	31	-262	-1.4
5°L	6.28	1.22	158	19	32	251	5.0

TABLE A-2. MODIFIED TARGET TRAJECTORY DATA
FOR THE LEFT EYE OF SUBJECT 2

SACCADE	DISPLACEMENT	IC	TP	TD	DUR	PV	DIST
5°L	4.4	.10	177	17	25	233	3.4
5°L	4.09	-.13	198	11	23	263	2.2
5°R	-4.35	-.16	165	12	23	-242	-2.6
5°L	4.01	-.31	193	10	21	242	2.4
5°R	-4.94	-.47	153	18	28	-237	-3.8
5°R	-5.05	.18	212	18	25	-280	-4.4
5°R	-4.32	-.16	175	18	34	-233	-2.9
5°L	3.24	-.34	194	13	28	229	1.6
5°L	4.04	-.31	230	9	21	229	1.3
5°R	-4.79	-.26	158	8	25	-203	-1.8
5°L	3.42	-.03	187	15	24	198	2.8
5°R	-4.09	-.05	224	15	28	-185	-2.7
5°R	-4.66	0.0	240	17	30	-237	-3.3
5°L	4.09	-.08	292	9	21	267	2.5

TABLE A-3. MODIFIED TARGET TRAJECTORY DATA
FOR THE LEFT EYE OF SUBJECT 3

SACCADE	DISPLACEMENT	IC	TP	TD	DUR	PV	DIST
5°L	5.44	1.05	207	10	29	213	2.9
5°L	5.29	1.16	197	14	26	252	3.7
5°R	-3.11	1.10	191	9	29	-252	-0.8
5°L	6.1	1.19	450	11	25	271	4.4
5°R	-2.99	1.6	204	16	28	-233	-1.2
5°R	-2.53	1.77	206	11	25	-247	-0.8
5°R	-3.63	1.74	198	21	31	-281	-2.3
5°L	6.51	2.15	171	15	27	218	4.6
5°L	6.43	2.24	212	11	21	286	4.8
5°R	2.56	-2.30	191	9	26	-213	0.6
5°L	6.25	2.56	156	15	27	208	5.1
5°R	2.41	-2.24	190	10	24	-262	-0.1
5°R	2.70	-1.34	229	9	32	-199	1.0
5°L	7.30	2.62	204	12	25	233	5.2

TABLE A-4. NORMAL SACCADIC DATA FOR SUBJECT 1

LEFT														RIGHT													
SACCADIC	DISPLACEMENT	IC	TD	DUR	TP	FV	DIST	DISPLACEMENT	IC	TD	DUR	TP	FV	DIST													
5°L	5.56	.80	17	26	195	289	4.5	5.64	.97	18	32	194	239	3.7													
5°L	6.19	.21	16	32	178	305	3.8	6.01	.26	21	48	177	268	4.3													
10°L	10.15	.28	17	39	182	379	5.0	11.15	.79	18	41	182	345	5.2													
10°L	10.39	.49	28	38	197	379	8.0	11.04	.57	18	42	198	319	4.2													
10°L	10.72	.66	19	40	199	371	6.5	11.15	.64	25	42	199	356	7.8													
15°L	14.26	.77	18	59	172	406	5.7	15.73	1.23	25	56	176	334	9.0													
15°L	14.33	.68	28	58	186	387	9.7	15.64	.66	21	56	187	389	6.4													
15°L	14.51	.59	21	53	212	418	6.9	15.94	.73	24	56	213	382	7.4													
5°R	-4.36	.91	16	34	163	-231	-1.8	-3.99	1.17	18	29	164	-246	-2.7													
5°R	-4.85	.59	23	34	171	-215	-3.6	-4.67	.70	19	36	169	-275	-3.2													
10°R	-9.1	.47	26	50	210	-297	-5.8	-8.63	.70	19	44	209	-356	-4.3													
10°R	-9.66	.33	19	49	131	-293	-4.3	-8.83	.59	23	50	127	-290	-4.8													
10°R		BAD RECORDS																									
15°R	-10.93	.77	24	70	182	-250	-4.8	-11.67	.81	20	67	180	-352	-4.5													
15°R	-11.25	.70	20	55	182	-340	-4.1	-11.28	.79	19	59	180	-374	-4.2													
15°R	-12.57	.52	35	66	183	-309	-6.8	-12.0	.59	19	58	186	-316	-4.2													

TABLE A-5. NORMAL SACCADDE DATA FOR SUBJECT 2

	LEFT					RIGHT									
	SACCADDE	DISPLACEMENT	IC	TD	DUR	TP	FV	DIST	DISPLACEMENT	IC	TD	DUR	TP	FV	DIST
5°L		3.61	- .99	18	29	174	207	1.8	4.72	.07	21	34	175	214	3.5
5°L		3.86	- .91	17	25	180	253	2.6	4.29	-.19	15	25	182	248	2.8
10°L		7.03	-1.14	18	37	176	341	2.9	8.98	.56	20	39	177	282	4.6
10°L		7.41	- .89	19	37	165	345	3.7	9.13	.26	20	39	165	304	4.6
10°L		8.52	- .76	28	37	215	341	7.0	9.57	.09	23	38	218	344	6.1
15°L		10.21	- .97	21	48	217	331	3.9	12.47	.13	27	47	221	338	7.5
15°L		10.3	-1.16	26	46	230	348	6.2	13.40	.54	25	54	227	313	6.0
15°L		11.27	-1.12	20	50	246	359		BAD DATA						
5°R		-5.30	-1.16	14	32	159	-204	-3.1	-4.46	.0	17	28	159	-239	-3.2
5°R		-5.30	-1.03	16	33	173	-211	-3.5	-4.33	.39	16	26	170	-273	-2.5
10°R		-10.38	- .95	24	38	168	-334	-6.9	-9.61	-.43	25	39	163	-347	-6.1
10°R		-10.55	-1.16	21	44	167	-299	-5.0	-9.57	-.19	26	40	167	-353	-7.1
10°R		-10.74	-1.05	25	35	173	-376	-8.4	-9.33	.07	23	31	171	-390	-7.2
15°R		-14.66	-1.05	28	43	183	-411	-10.4	-11.69	.11	19	41	181	-406	-6.3
15°R		-14.7	- .65	21	44	200	-415	-6.6	-12.06	.11	20	37	201	-418	-7.0
15°R		-15.51	- .86	23	52	211	-352	-6.5	-12.58	.13	22	49	211	-390	-6.4

TABLE A-6. NORMAL SACCADE DATA FOR SUBJECT 3

SACCADE	LEFT				RIGHT				IC	TD	DUR	TP	PV	DIST	DISPLACEMENT	IC	TD	DUR	TP	PV	DIST
	DISPLACEMENT	IC	TD	DUR	TP	PV	DIST	DISPLACEMENT													
5°L	6.14	2.45	15	38	165	179	4.1	4.65	.17	15	41	167	194	1.9							
5°L	6.98	1.71	20	28	185	286	5.4	5.98	.06	20	26	191	248	4.9							
10°L	10.62	.95	21	38	205	401	6.2	10.2	.43	18	34	209	391	5.6							
10°L	10.9	2.0	21	43	203	329	6.8	10.08	.22	22	45	203	323	5.5							
10°L	11.00	2.26	23	39	169	357	8.1	10.10	.34	21	42	169	344	5.4							
15°L	12.90	2.69	22	45	174	373	7.6	12.03	.15	23	50	173	377	4.9							
15°L	14.88	2.07	23	45	177	397	8.8	13.91	.30	22	52	176	420	6.1							
15°L	15.38	2.12	21	52	194	385	7.6	14.53	.41	21	52	194	402	6.1							
5°R	-2.43	2.62	21	40	170	-254	0.0	-4.50	.26	24	39	169	-262	-3.2							
5°R	-3.6	1.86	19	33	182	-254	-2.1	-5.27	.09	17	31	179	-312	-3.2							
10°R	-6.95	2.38	29	44	169	-357	-5.0	-8.20	.19	21	42	169	-341	-4.9							
10°R	-8.02	1.79	20	38	193	-389	-4.2	-9.24	0.00	23	42	187	-395	-5.4							
10°R	-9.43	1.6	24	43	190	-341	-4.6	-10.09	.09	17	39	189	-337	-4.1							
15°R	-11.6	1.86	23	44	310	-437	-5.7	-11.93	.13	26	42	308	-398	-8.2							
15°R	-11.95	2.14	22	55	168	-409	-3.6	-10.64	.54	21	46	167	-427	-5.2							
15°R	-12.17	2.12	25	54	169	-417	-4.2	-11.52	.32	22	47	170	-434	-6.1							

END

FILMED

10-85

DTIC